

Experimental verification of algorithms for detection and estimation of radioactive sources

Ajith Gunatilaka

HPP Division

DSTO

Australia

ajith.gunatilaka@dsto.defence.gov.au

Branko Ristic

ISR Division

DSTO

Australia

branko.ristic@dsto.defence.gov.au

Mark Morelande

MSL, Dept EEE

The University of Melbourne

Australia

mmorelande@unimelb.edu.au

Abstract – *The paper considers the problem of estimating the number of radioactive point sources that potentially exist in a designated area and estimating the parameters of these sources (their locations and strengths) using measurements collected by a low-cost Geiger-Müller counter. In a recent publication the authors proposed candidate algorithms for this task: the maximum likelihood estimator (MLE) and the importance sampling estimator based on progressive correction (PC) for source parameter estimation, and the minimum description length (MDL) for the estimation of the number of sources. Using real experimental data acquired during a recent radiological field trial in Puckapunyal Military Area (Victoria, Australia), in the presence of up to three point sources of gamma radiation, this paper presents an experimental verification of the measurement model and algorithms proposed by us earlier. These experimental results show that while the MLE performs well when no more than two sources are present, the PC performs remarkably well for all data sets, which confirms our previous conclusions based on simulation studies alone.*

Keywords: Bayesian estimation. Gamma radiation, radiological instruments, experimental verification.

1 Introduction

Numerous incidents involving a loss or theft of radioactive sources have been reported [1]. There is growing concern that these sources could end up in the hands of terrorist networks and be used for building radiological dispersion devices. The ability to rapidly localise sources of gamma radiation can assist emergency responders to disable, isolate or safely remove such devices. In this paper we are primarily interested in radiological materials that emit gamma rays, the highly penetrating electromagnetic radiations that can travel large distances through air.

Detection and localisation of point-sources of gamma radiation have been studied recently by several authors. For example, [2, 3, 4] consider detection of moving radiation sources using networks of radiation sensors. Detection of radiation sources using coded apertures or Compton imaging is considered in [5] and [6]. Radiation field estimation using Gaussian mixtures is examined in [7]. In this paper we focus on the specific problem and algorithms presented in [8], which considers the estimation of the number of gamma radiation point sources in an area and determination of their locations and strengths using measurements acquired at arbitrary but precisely known positions using a low-cost Geiger-Müller (GM) counter. While emerging technologies such as coded apertures may become affordable and practical for locating gamma sources in the future, the present work concerns the use of measurements from low-cost, hand held radiation detectors currently fielded by military emergency responders for source localisation.

For estimation of source parameters (assuming their number is known), two algorithms are considered [8]: the maximum likelihood estimator (MLE), which requires optimisation over the parameter space and a Bayesian estimator implemented using a Monte Carlo importance sampling with progressive correction (PC). Simulation based studies in [8] concluded that in the presence of more than two sources, optimisation required by the MLE becomes problematic, consequently making this algorithm unreliable. The Bayesian estimator with PC, on the contrary, was able to perform accurate source parameter estimation even in the presence of three or four sources. The estimation error performance was compared with the theoretical Cramér-Rao bound (CRB), which defines the best achievable error performance. Estimation of the number of sources (order selection) was carried out using the minimum description length (MDL).

In this paper we experimentally verify the observations and conclusions made in [8]. Real data sets ac-

quired during a field trial in Puckapunyal Military Area (Victoria, Australia) are used in the study. The data sets were collected using the DSTO-developed Low Cost Advanced Radiological Survey (LCAARS) system in the presence of one, two, and three radiological point sources of unequal strengths. An additional data set was recorded in the absence of any sources, so that the average background radiation can be estimated. The designated area was a polygon with the longest sides less than 100m long. The paper presents the CRB analysis, the parameter estimation, and the results of the estimation of the number of sources using the MLE and the PC for all three data sets.

The organisation of the paper is as follows. Section 2 describes the measuring model and formulates the problem. Section 3 describes the three experimental data sets. Section 4 reviews the theory from [8]: the CRB, the MLE and the PC for the estimation of source parameters, as well as the MDL for the estimation of the number of sources. Section 5 presents the numerical results and Section 6 draws the conclusions.

2 Problem formulation and modelling

The radiation counts from nuclear decay obey Poisson statistics [9, 10]: the probability that a gamma radiation detector registers $z \in \mathbb{N}$ counts (\mathbb{N} being the set of natural numbers *including* zero) in τ seconds, from a source that emits on average μ counts per second is:

$$\mathcal{P}(z; \lambda) = \frac{\lambda^z}{z!} e^{-\lambda}, \quad (1)$$

where $\lambda = \mu\tau$ is the parameter (both the mean and the variance) of the Poisson distribution.

Assume that $r \geq 0$ sources are present in an area of interest (which in this study is assumed to be flat without obstacles). The number of sources, r , is unknown. The case $r = 0$ corresponds to the absence of any radiation sources, while for $r > 0$, each point source of gamma radiation i (where $i = 1, 2, \dots, r$) is parameterised by

- Its location (x_i, y_i) in the Cartesian coordinate system;
- Its equivalent strength, α_i , which is a single parameter that takes into account the activity of the radioactive source, the value of gamma energy per disintegration and the scaling factors involved [11]. How this quantity was determined in the field trials is described in Sec.3.

The parameter vector of source i is thus given by:

$$\boldsymbol{\theta}_i = [x_i \quad y_i \quad \alpha_i]^\top, \quad (2)$$

where \top denotes the matrix transpose. The source parameter vectors are collected into a stacked vector $\boldsymbol{\theta} = [\boldsymbol{\theta}_1^\top \quad \dots \quad \boldsymbol{\theta}_r^\top]^\top$.

The measurements of radiation field are made using a GM counter. Let $z_j \in \mathbb{N}$, where $j = 1, \dots, m$, be a measured count from the GM counter, taken at location $(\xi_j, \zeta_j) \in \mathbb{R}^2$. The following assumptions are made: (1) the GM counter has a uniform directional response; (2) radiation sources are point sources; (3) there is negligible attenuation of gamma radiation due to air; (4) radiation measurements are independently distributed; (5) the exposure time (i.e. the sampling interval) is constant for all measurements. The joint density of the measurement vector $\mathbf{z} = [z_1 \quad \dots \quad z_m]^\top$ conditional on the parameter vector $\boldsymbol{\theta}$ and the knowledge that r sources are present, can then be written as a product of Poisson distributions [11, 9]

$$l(\mathbf{z}|\boldsymbol{\theta}) = \prod_{j=1}^m \mathcal{P}(z_j; \lambda_j(\boldsymbol{\theta})), \quad (3)$$

where $\lambda_j(\boldsymbol{\theta})$ is the mean radiation count for the j th sensor location:

$$\lambda_j(\boldsymbol{\theta}) = \lambda_b + \sum_{i=1}^r \frac{\alpha_i}{d_{ji}^2}, \quad (4)$$

with

$$d_{ji} = \sqrt{(\xi_j - x_i)^2 + (\zeta_j - y_i)^2} \quad (5)$$

being the distance between the source i and the j th sensor.

The described measurement model is based on two assumptions which need further explanation. First, λ_b in (4) which represents the *average count* due to the background radiation only, is assumed to be a known constant. This assumption may not hold in general (especially in an urban environment) [12]. However, repeated measurements of background radiation of the field trial site showed that λ_b indeed had little temporal and spatial variation. Second, the model in (4) assumes that attenuation of gamma radiation due to air is negligible. In reality, this is not the case and the term inside the summation of (4) should be multiplied by an attenuation factor of the form $e^{-\beta d_{ji}}$, where β represents the air absorption coefficient. However, since the field trial involved measurements taken at relatively short distances (less than 100m), we approximate the exponential term as $e^{-\beta d_{ji}} \approx 1$.

The problem is to estimate r and the parameter vector $\boldsymbol{\theta}$ using the measurement vector \mathbf{z} , and the measurement model given by (3)–(5).

3 Experimental setup and calibration

A radiological field trial was conducted on a large, flat, and open area without any obstacles. The LCAARS survey system consists of an AN/PDR-77 radiation survey meter equipped with an RS232 interface

module, a gamma probe and software written in Visual Basic and running on a laptop computer. The gamma probe contains two Geiger-Müller tubes to cover both low and high ranges of dose rates and, when connected to the AN/PDR-77 radiation survey meter, it is capable of measuring gamma radiation dose rates from background to 9.99 Sv/h without saturating [13]. The gamma probe has a fairly flat response ($\sim \pm 10\%$) from 0.1 to above 1MeV [13, pg. 7]. Measured dose rate data were recorded in $\mu\text{Sv/h}$. We converted these data into raw count measurements $z_j \in \mathbb{Z}^+$ by multiplication with a conversion factor (which was 1/0.21 for our probe). The measured normalised directional response pattern of the gamma probe (mounted vertically) is shown in Figure 1. This concerns our first assumption in Sec.2, which is approximately satisfied in the horizontal 2D plane.

Three radiation sources were used in the field trial: two cesium sources (^{137}Cs) and one cobalt (^{60}Co) source (see Table 1). While the strengths of radiation sources are typically characterised in terms of their activity in GBq, as shown in Table 1, in this work, for simplicity, we characterise the strength of a radiation point source by the expected count rate at a distance of 1m from the source. The strengths of our three radiation sources calibrated in this manner were 9105, 1868 and 467, for Sources 1, 2 and 3, respectively. We will use these values as the “true” source strength values in the computation of the CRBs and in the computation of the root-mean-squared (RMS) estimation errors. The sources were mounted at the same height above the ground as the gamma probe. To ensure that radiation sources appear as isotropic, they were placed in a vertical configuration such that the handling rods were pointing up.

Table 1: *Radiation sources used in the field trial*

Source	Type	Activity (MBq)
1	^{137}Cs	26×10^3
2	^{137}Cs	5×10^3
3	^{60}Co	0.2×10^3

Radiation dose measurements were collected in grid points that were carefully measured and marked beforehand in the local Cartesian coordinate system on the asphalt surface of the airfield. The data were acquired when the trolley-mounted gamma probe was positioned over individual grid points. During data collection at any grid point, the gamma probe was held stationary until approximately sixty measurements were acquired. The exposure time for each radiation dose measurement (effectively the sampling interval τ) was kept constant at about 0.8 seconds. Multiple measurements are collected at each location so that the candidate algorithms

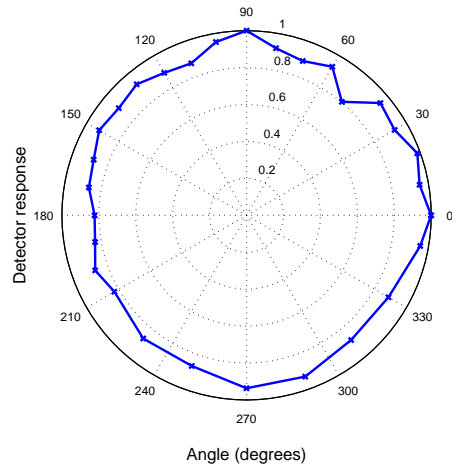


Figure 1: *Normalised directional response pattern of the gamma probe.*

can be tested using several different batches of experimental data¹.

Data sets were collected with one, two, and three radiation sources emplaced, respectively. These data sets are referred to as Test set 1, 2 and 3. The sources used when collecting these data sets and their locations in the local Cartesian coordinate system for are listed in Table 2.

Table 2: *The locations of radiation sources in the field trial*

Test set	Source 1 Location	Source 2 Location	Source 3 Location
1	(11, 10)m	-	-
2	(11, 10)m	(3, 50)m	-
3	(11, 10)m	(3, 50)m	(41, 5)m

The areal picture of the Puckapunyal airfield site where the field trial was conducted is shown in Figure 2. The three green stars show the locations where the three radiation sources were emplaced. The white cross symbols indicate the grid points where data were collected. The X and Y axis markings on the plot show the distances along these directions in meters.

In order to estimate the background radiation level in the field trial, measurements were collected at a number of grid positions in the *absence* of radiations sources. At each of these grid positions, the detector was held stationary until 120 measurements were acquired. The background radiation was found to be Poisson with mean $\lambda_b \approx 0.9$ counts.

¹Manual measurement of sensor locations can be replaced by differential GPS positioning, with data being acquired continuously as the sensor traverses the search area.

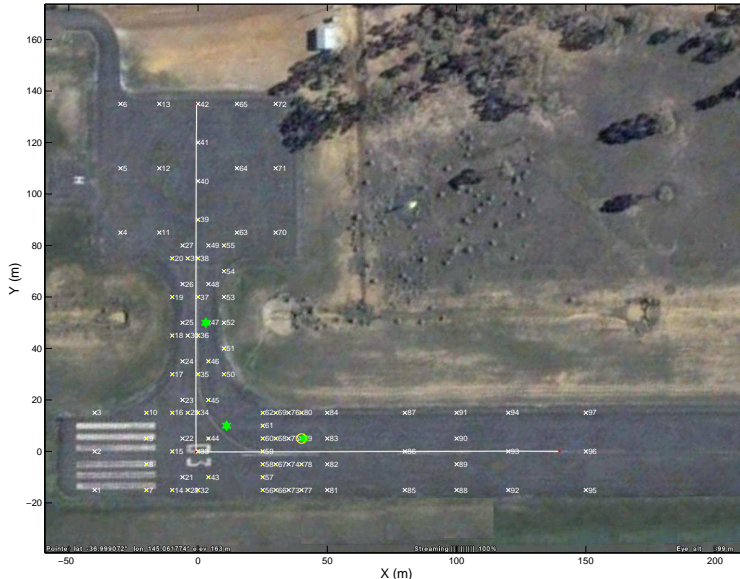


Figure 2: Aerial image of the Puckapunyal airfield site where the field trial was conducted. The green stars located at coordinates $(11, 10)m$, $(3, 50)m$ and $(41, 5)m$ of the local Cartesian coordinate system indicate where the three sources were emplaced for Test 3. The numbered grid points marked with crosses are the measurement points.

4 Estimation algorithms

This section reviews the candidate estimation algorithms and the theoretical estimation error bound.

4.1 Cramér-Rao bound

In many estimation problems optimal parameter estimates can be found only through the use of numerical techniques, the reliability of which cannot be guaranteed. Theoretical error performance bounds provide a way of assessing these numerical techniques even before any measurements are collected. The most popular performance bound is the Cramér-Rao bound which places a lower bound on the variance of unbiased estimators. In particular, for an unbiased estimator $\hat{\boldsymbol{\theta}}$ of the deterministic parameter vector $\boldsymbol{\theta}$ the CRB for $\text{cov}(\hat{\boldsymbol{\theta}})$ is \mathbf{J}^{-1} where \mathbf{J} is the Fisher information matrix (FIM) [14, p.80],

$$\mathbf{J} = -\mathbb{E}[\nabla_{\boldsymbol{\theta}} \nabla_{\boldsymbol{\theta}}^T \log l(\mathbf{z}|\boldsymbol{\theta})] \quad (6)$$

with $\mathbb{E}[\cdot]$ the expectation, $\nabla_{\boldsymbol{\theta}}$ the gradient operator with respect to $\boldsymbol{\theta}$ and $l(\mathbf{z}|\boldsymbol{\theta})$ the likelihood function of the measurement vector \mathbf{z} given by (3). The CRB holds in the sense that $\text{cov}(\hat{\boldsymbol{\theta}}) - \mathbf{J}^{-1}$ is positive semidefinite.

It has been shown in [8] that for the measurement model (3)–(5), the FIM can be expressed as:

$$\mathbf{J} = \sum_{j=1}^m \frac{\nabla_{\boldsymbol{\theta}} \lambda_j(\boldsymbol{\theta}) \nabla_{\boldsymbol{\theta}}^T \lambda_j(\boldsymbol{\theta})}{\lambda_j(\boldsymbol{\theta})}. \quad (7)$$

where the partial derivatives in $\nabla_{\boldsymbol{\theta}} \lambda_j(\boldsymbol{\theta})$ can be found

as

$$\frac{\partial \lambda_j(\boldsymbol{\theta})}{\partial x_i} = 2\alpha_i (\xi_j - x_i) / d_{ji}^4, \quad (8)$$

$$\frac{\partial \lambda_j(\boldsymbol{\theta})}{\partial y_i} = 2\alpha_i (\zeta_j - y_i) / d_{ji}^4, \quad (9)$$

$$\frac{\partial \lambda_j(\boldsymbol{\theta})}{\partial \alpha_i} = 1 / d_{ji}^2. \quad (10)$$

for $i = 1, \dots, r$ and $j = 1, \dots, m$.

The theoretical Cramér-Rao bounds are computed as diagonal elements of \mathbf{J}^{-1} for Tests 1, 2 and 3. The square-root values (which correspond to the lower bounds of estimation error standard deviations) are shown in the first columns of Tables 4, 5 and 6. The resulting bounds indicate that it is possible in all three experimental tests to accurately localise the sources (with standard deviation of the positional error in the order of a meter). The bounds also indicate that estimation of source strengths can be carried out fairly accurately.

4.2 Estimation of $\boldsymbol{\theta}$ using the MLE

The MLE is widely used for parameter estimation because, if an asymptotically unbiased and minimum variance estimator exists for large sample sizes, it is guaranteed to be the MLE [14]. When estimating source parameters we implicitly assume that we know the number of sources. The MLE is determined as the vector $\boldsymbol{\theta}$ which maximises the likelihood function $l(\mathbf{z}|\boldsymbol{\theta})$ given by (3):

$$\hat{\boldsymbol{\theta}}_{\text{ML}} = \arg \max_{\boldsymbol{\theta}} l(\mathbf{z}|\boldsymbol{\theta}). \quad (11)$$

This is equivalent to finding θ for which gradient $\nabla_{\theta} \lambda_k(\theta)$ equals zero. In the absence of the analytical solution we carry out maximisation in (11) numerically. This is done by minimisation of the negative log-likelihood function, i.e.

$$\hat{\theta}_{\text{ML}} = \arg \min_{\theta} \{-\log l(\mathbf{z}|\theta)\} \quad (12)$$

where minimisation is performed using the Nelder-Mead method [15] implemented as the MATLAB built-in routine *fminsearch*. The main problem with the minimum search is that, depending on the initial value, it may find a local rather than the global minimum, resulting in a wrong estimate. This problem may be avoided to some extent by repeating the search a number of times using different initial values and then choosing the best solution.

4.3 Estimation of θ using the PC

The progressive correction is a Bayesian technique which assumes that a prior distribution $\theta \sim \pi_0(\theta)$ is available for source parameter estimation. The information contained in the measurements is combined with the prior information to give the posterior probability density function (PDF),

$$\pi(\theta|\mathbf{z}) \propto l(\mathbf{z}|\theta)\pi_0(\theta). \quad (13)$$

The minimum mean squared error (MMSE) estimate of θ is then the posterior expectation,

$$\hat{\theta}_{\text{B}} = \mathbb{E}(\theta|\mathbf{z}) = \int \theta \pi(\theta|\mathbf{z}) d\theta. \quad (14)$$

The posterior π , and hence the posterior expectation, cannot be found exactly for the measurement model of Section 2. Instead an approximation of (14) is computed via importance sampling: it involves drawing N samples of the parameter vector from an importance density and approximating the integral by a weighted sum of the samples. Details are given in [8] and [16]. Here we point out that PC is a multi-stage procedure in which samples are obtained from a series of posterior distributions which become progressively closer to the true posterior distribution. This is achieved by adopting an approximate likelihood which is somewhat more diffuse than the true likelihood.

Let S denote the number of stages and π_s , $s = 1, \dots, S$ denote the posterior PDF at stage s (note that $\pi_S = \pi$). A series of π_s which satisfy the requirements of the previous paragraph can be constructed by setting

$$\pi_s(\theta|\mathbf{z}) \propto l_s(\mathbf{z}|\theta)\pi_0(\theta) \quad (15)$$

where the intermediate likelihood at stage $s = 1, \dots, S$ is $l_s(\mathbf{z}|\theta) = l(\mathbf{z}|\theta)^{G_s}$ with $G_s = \sum_{\ell=1}^s \gamma_{\ell}$, such that $\gamma_s \in [0, 1]$, and $G_S = 1$. Assume that a random sample $\{w^n, \theta^{s-1,n}\}$ from π_{s-1} is available and it is desired

to produce a sample from π_s . The steps of the PC algorithm are given in Table 3. Note that for $s = 1$, the sample $\{w^n, \theta^{s-1,n}\}$ is drawn directly from prior π_0 with $w^n = 1/N$.

Table 3: Importance sampling with progressive correction algorithm

```

1:  $s = 0, G_0 = 0;$ 
2: for  $n = 1, \dots, N$  do
3:   Draw  $\theta^{0,n} \sim \pi_0$ 
4:   Compute  $l(\mathbf{z}|\theta^{0,n})$ 
5: end for
6: while  $G_s < 1$  and  $s < S$  do
7:    $s \leftarrow s + 1$ 
8:   Select  $\gamma_s$ 
9:    $G_s = G_{s-1} + \gamma_s$ 
10:  for  $n = 1, \dots, N$  do
11:    Weights:  $w^{s,n} = l(\mathbf{z}|\theta^{s-1,n})^{\gamma_s} / \sum_{j=1}^N l(\mathbf{z}|\theta^{s-1,n})^{\gamma_s}$ 
12:  end for
13:  Resample according to weights  $w^{s,1}, \dots, w^{s,N}$ 
14:  for  $n=1, \dots, N$  do
15:     $\theta^{s,n} = \theta^{s-1,n} + \epsilon^{s,n}$ , where  $\epsilon \sim g_s$ 
16:  end for
17: end while

```

The performance of the procedure depends somewhat on the number of steps S and the expansion factors $\gamma_1, \dots, \gamma_S$. The expansion factors γ_s were selected in line 8 of Table 3 using an adaptive scheme proposed in [16]. In this adaptive scheme the expansion factors are selected after each step rather than being selected *a priori*. Line 15 in Table 3 performs regularisation (jittering) of samples in order to avoid their duplication; g_s is a Gaussian regularisation kernel [16]. The final PC estimate (14) is approximated as:

$$\hat{\theta}_{\text{B}} = \frac{1}{N} \sum_{n=1}^N \theta^{S,n} \quad (16)$$

4.4 Source number estimation

Both estimation techniques assume that the number of sources is known *a priori*. In practice, however, this number too needs to be estimated from the data (this type of a problem is referred to as the *model order selection*). The conventional solution to this problem is the so called generalised maximum likelihood (GML) rule [17, p.223]. Let \mathcal{M} denote a set of candidate source numbers. For example, if we wish to test for all source numbers up to some maximum r_{max} , then $\mathcal{M} = \{0, \dots, r_{\text{max}}\}$. It is desired to determine which of the source numbers in \mathcal{M} best fits a given collection of measurements \mathbf{z} . This is done by maximising for $r \in \mathcal{M}$ the following quantity:

$$\beta_r = \log p(\mathbf{z}|\hat{\theta}_{\text{ML},r}) - \frac{1}{2} \log |\mathbf{J}(\hat{\theta}_{\text{ML},r})|, \quad (17)$$

where $\hat{\theta}_{\text{ML},r}$ is the MLE under the assumption that r sources are present and $\mathbf{J}(\theta)$ is the Fisher information

matrix derived in Section 4 evaluated for the parameter value θ . A useful approximation of the GML rule is the minimum description length (MDL) which chooses the value of r that minimises [17, pg. 225],[18]:

$$\mu_r = -\log l(\mathbf{z}|\hat{\theta}_{\text{ML},r}) + \frac{n_r}{2} \log m \quad (18)$$

where n_r is the dimension of θ under the hypothesis $r \in \mathcal{M}$. The estimate of the number of sources r is then computed as:

$$\hat{r} = \arg \min_{r \in \mathcal{M}} \mu_r. \quad (19)$$

The MDL is derived based on the MLE estimate $\hat{\theta}_{\text{ML}}$, see (18). We will use the MDL for the PC too, by simply replacing $\hat{\theta}_{\text{ML}}$ with the PC estimate $\hat{\theta}_{\text{B}}$ in (18).

5 Numerical results

5.1 Implementation details

We assume that $r \in \mathcal{M}$ sources are located in a specified polygon-shaped area \mathcal{A} . The polygon typically contains all measurement points. The prior PDF for source location is then a uniform density with limits specified by \mathcal{A} , which we denote by $\mathcal{U}[\mathcal{A}(x_i, y_i)]$. The initial source strength value is drawn from a Gamma distribution $\Gamma_{\kappa, \nu}(\alpha)$ with shape parameter $\kappa = 1.5$ and scale parameter $\nu = 8000$. This prior distribution was chosen because it is broad enough to cover all likely source strength values (in counts). Thus our prior PDF for a source $i = 1, \dots, r$ can be written as:

$$\pi_0(\theta_i) = \mathcal{U}[\mathcal{A}(x_i, y_i)] \cdot \Gamma_{\kappa, \nu}(\alpha_i) \quad (20)$$

and for the stacked parameter vector $\pi_0(\theta) = \prod_{i=1}^r \pi_0(\theta_i)$.

The MLE strictly speaking does not use prior information, however we initialise the minimum search routine with $\theta^0 \sim \pi_0(\theta)$.

The PC is initialised by drawing a random sample in $3r$ dimensional parameter space from $\pi_0(\theta)$. The number of samples in the PC is set to $N = 2500r$.

The expansion factors and the actual number of stages of the PC are data dependent. We have tuned the PC so that on average the number of stages is directly proportional to the number of sources.

In order to improve the performance, both MLE and the PC consist of multiple runs on each data set. The minimum search in the MLE is performed 5 times with different random initial values, and the run which resulted in the smallest negative log-likelihood (12) is selected as the correct MLE estimate (in this way we reduce the chance of finding a local instead of the global minimum in optimisation). The separate instances of the PC are performed on the same measurements until the final spread of random samples in the $x - y$ plane falls below a certain threshold. Thus after stage S we

compute not only the estimate $\hat{\theta}_{\text{B}}$ in (16), but also its sample covariance matrix Σ . Suppose the diagonal elements of Σ are $\sigma_{x_1}^2, \sigma_{y_1}^2, \sigma_{\alpha_1}^2, \sigma_{x_2}^2$, etc. Then the criterion for PC termination is that

$$\sum_{i=1}^r \sqrt{\sigma_{x_i}^2 + \sigma_{y_i}^2} \leq 2.5r. \quad (21)$$

Figure 3 shows four stages ($s = 1, 2, 4$ and 11) of a typical run of the PC for Test 3 data set. The specified polygon area \mathcal{A} is plotted in green. There are three colours of random samples, one for each source. Blue circles indicate the positions and magnitudes of count measurements. The three red asterisks show the true source locations (see Table 2). We observe that samples concentrate most rapidly around Source 3 (and in this case they are orange coloured) due to the strong measurement taken in the vicinity of this source. The slowest is the convergence of samples towards Source 2, because all measurements around this source are fairly weak.

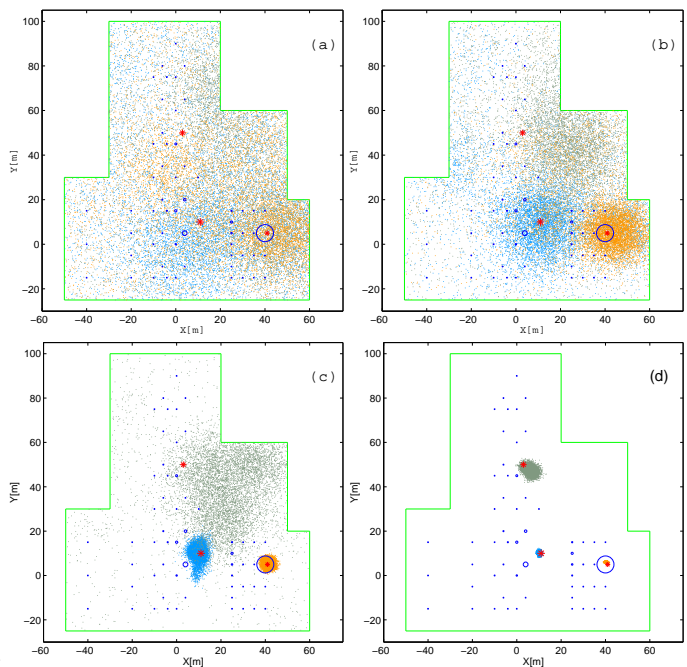


Figure 3: A single run of the progressive correction estimator - Test 3 data set: (a) after stage $s = 1$, (b) after stage $s = 2$, (c) after stage $s = 4$ and (d) after stage $S = 11$ (the final stage for this run).

5.2 Parameter estimation results

Recall that for each test data set, we have in each measurement location approximately 60 independent count measurements. This enables us to perform multiple runs and obtain average error performance using the real data from all three data sets. Next we define the criterion for a divergent run. Let the CRB of source

$i = 1, \dots, r$ for position in x and y be denoted as C_{x_i} , C_{y_i} , respectively. A run is declared divergent if for any $i = 1, \dots, r$ the positional estimation error is five or more times higher than the positional error predicted by the CRB, that is:

$$\sqrt{(x_i - \hat{\theta}_i[1])^2 + (y_i - \hat{\theta}_i[2])^2} \geq 5\sqrt{C_{x_i}^2 + C_{y_i}^2}. \quad (22)$$

where $\hat{\theta}_i[1]$ and $\hat{\theta}_i[2]$ denote the estimated position of source i in x and y coordinates, respectively.

Tables 4, 5 and 6 list the number of divergent runs and the RMS errors of non-divergent runs, for all three data sets. Overall the results indicate good performance and validate the measurement model in Section 2. For the single source case (see Table 4) we conclude that both the MLE and the PC perform quite well, with no divergent runs and with the RMS errors only slightly higher than the theoretical CRB.

We point out that the CRBs were computed based on our idealized measurement model, which as we have seen is based on many assumptions and approximations (e.g. uniform directional response, neglected air attenuation, perfect knowledge of sensor locations, known and constant average background λ_b , etc). Therefore the CRBs should be seen only as a guideline for achievable accuracy; in general they are too optimistic.

Table 4: *Test 1 data set (single source): RMS estimation error ($M = 50$ runs)*

	$\sqrt{\text{CRB}}$	RMSE-MLE	RMSE-PC
no. diverg.	-	0	0
x_1 [m]	0.30	0.48	0.50
y_1 [m]	0.43	0.51	0.60
α_1 [$\mu\text{Sv/h}$]	64	67	84

For Test 2 data set, with two sources present (see Table 5), we make a similar observation: both the MLE and the PC performed reasonably well with RMS errors only slightly higher than the CRBs. The MLE, however, diverged on two occasions.

Table 5: *Test 2 data set (two sources): RMS estimation error ($M = 50$ runs)*

	$\sqrt{\text{CRB}}$	RMSE-MLE	RMSE-PC
num.diverg.	-	2	0
x_1 [m]	0.30	0.52	0.50
y_1 [m]	0.45	0.64	0.69
α_1 [$\mu\text{Sv/h}$]	72	117	134
x_2 [m]	1.50	1.99	1.82
y_2 [m]	0.62	1.13	1.43
α_2 [$\mu\text{Sv/h}$]	82	124	107

Finally, the results for Test 3 (Table 6) indicate that the MLE is not a suitable algorithm in the presence of three sources: it diverged on every single run. The PC, on the other hand, performed remarkably well even in this case: the RMS localisation errors were approximately 1m, and again similar to the CRBs. Even on the two divergent runs of the PC, it estimated accurately the parameters for sources 1 and 3, but localised source 2 with an error of about 10m.

Table 6: *Test 3 data set (three sources): RMS estimation error ($M = 50$ runs)*

	$\sqrt{\text{CRB}}$	RMSE-MLE	RMSE-PC
no.diverg.	-	50	2
x_1 [m]	0.35	-	0.62
y_1 [m]	0.46	-	0.57
α_1 [$\mu\text{Sv/h}$]	85	-	160
x_2 [m]	1.12	-	2.6
y_2 [m]	0.57	-	1.48
α_2 [$\mu\text{Sv/h}$]	63	-	195
x_3 [m]	0.20	-	1.27
y_3 [m]	2.66	-	1.02
α_3 [$\mu\text{Sv/h}$]	39	-	95

5.3 Results for the estimation of r

Since the MLE is not suitable for Test 3 data set, when using the MLE in MDL (18), we assumed that the set of candidate models for r is $\mathcal{M} = \{0, 1, 2\}$. Table 7 shows the number of runs (out of $M = 50$) which resulted in a source number r . The results indicate fairly accurate detection performance of the MLE based MDL detector.

Table 7: *Estimation of the source number using the MLE in MDL (18). Table lists the number of runs (out of $M = 50$) that resulted in $r \in \{0, 1, 2\}$*

Test data set	True r	Estimated \hat{r}		
		0	1	2
Background	0	50	0	0
test 1	1	0	50	0
test 2	2	0	4	46

Finally Table 8 presents the results in estimation of the number of sources r using the PC estimate in MDL (18) and the set of candidate models $\mathcal{M} = \{0, 1, 2, 3\}$. We observe that the source number is estimated with high accuracy particularly for Tests 1 and 2.

6 Conclusions

The paper presented the results in estimation of the number of gamma radiation sources and their param-

Table 8: *Estimation of the source number using the PC in MDL (18). Table lists the number of runs (out of $M = 50$) that resulted in $r \in \{0, 1, 2, 3\}$*

Test data set	True r	Est. \hat{r}			
		0	1	2	3
Backgr.	0	50	0	0	0
Test 1	1	0	48	2	0
Test 2	2	0	0	49	1
Test 3	3	0	0	6	44

eters using experimental data sets collected in a recent field trial. The experimental setup included up to three sources (two cesium and one cobalt) of different strengths, with measurements collected by a low-cost Geiger-Müller counter. Overall the estimation results are in agreement with the simulation studies carried out earlier: the progressive correction estimator performs remarkably well for all data sets.

The analysis presented in the paper is important because it serves as an experimental verification of a fairly simple measurement model, which was based on several assumptions and approximations. The numerical results indicate a modest cumulative effect of modelling inaccuracies to the estimation error performance. The contribution of modelling errors is quantified by the difference between the theoretical RMS errors (computed via the Cramér-Rao bounds) and the actual RMS errors.

Future work will consider ways to relax the simplifying assumptions made in the present work (e.g. robustness to nonhomogeneous background radiation, presence of obstacles, etc) so that source localisation can be achieved in more realistic scenarios.

Acknowledgment

The authors would like to thank their DSTO colleagues A. Skvortsov, R. Gailis, A. Eleftherakis, D. Marinaro, P. Harty and I. Mitchell for useful technical discussions and their involvement in the field trial.

References

- [1] W. K. H. Panofsky, "Nuclear proliferation risks, new and old," *Issues in Science and Technology*, vol. 19, 2003, <http://www.issues.org/19.4/panofsky.html>.
- [2] R. J. Nemzek, J. S. Dreicer, D. C. Torney, and T. T. Warnock, "Distributed sensor networks for detection of mobile radioactive sources," *IEEE Trans. Nuclear Science*, vol. 51, no. 4, pp. 1693–1700, 2004.
- [3] D. L. Stephens and A. J. Peurrung, "Detection of moving radioactive sources using sensor networks," *IEEE Trans. Nuclear Science*, vol. 51, no. 5, pp. 2273–2278, 2004.
- [4] S. M. Brennan, A. M. Mielke, and D. C. Torney, "Radioactive source detection by sensor networks," *IEEE Trans. Nuclear Science*, vol. 52, no. 3, pp. 813–819, 2005.
- [5] K. P. Ziock, L. Fabris, D. Carr *et al.*, "A fieldable-prototype, large-area, gamma-ray imager for orphan source search," *IEEE trans. Nucl. Sci.*, vol. 55, no. 6, pp. 3643–3653, 2008.
- [6] C. G. Wahl and Z. He, "Sensitivity of gamma-ray source detection using 3d-position-sensitive semiconductor detectors," in *IEEE Nucl. Sci. Symp.*, 2008, pp. 3334–3338.
- [7] M. Morelande and A. Skvortsov, "Radiation field estimation using a gaussian mixture," in *Proc. Int. Conf. Information Fusion*, Seattle, WA, USA, 2009.
- [8] M. Morelande, B. Ristic, and A. Gunatilaka, "Detection and parameter estimation of multiple radioactive sources," in *Proc. Int. Conf. Information Fusion*, Québec, Canada, 2007.
- [9] N. Tsoulfanidis, *Measurement and detection of radiation*. Washington, DC : Taylor & Francis, 1995.
- [10] A. V. Klimenko, W. C. Priedhorsky, N. W. Hengartner, and K. N. Borozin, "Efficient strategies for low-level nuclear searches," *IEEE Trans. Nuclear Science*, vol. 53, no. 3, pp. 1435–1442, June 2006.
- [11] A. Martin and S. A. Harbison, *An introduction to radiation protection*. Chapman & Hall, 1987.
- [12] K.-P. Ziock and K. E. Nelson, "Maximum detector sizes required for orphan source detection," *Nuclear Instruments and Methods in Physics Research*, vol. 579, p. 357362, 2007.
- [13] *AN/PDR-77 User's Guide*, Canberra Industries Inc., CT, USA.
- [14] H. L. V. Trees, *Detection, Estimation and Modulation Theory (Part I)*. John Wiley & Sons, 1968.
- [15] W. H. Press, B. P. Flannery, S. A. Teukolsky, and W. T. Vetterling, *Numerical recipes in C*, 2nd ed. Cambridge Univ. Press, 1992.
- [16] C. Musso, N. Oudjane, and F. LeGland, "Improving regularised particle filters," in *Sequential Monte Carlo methods in Practice*, A. Doucet, N. deFreitas, and N. J. Gordon, Eds. New York: Springer-Verlag, 2001.
- [17] S. M. Kay, *Statistical Signal Processing: Detection theory*. Prentice Hall, 1998.
- [18] J. Rissanen, "Modelling by shortest data description," *Automatica*, vol. 14, pp. 465–471, 1978.